JOURNAL OF GUIDANCE, CONTROL, AND DYNAMICS
Vol. 28, No. 5, September–October 2005

Globally Stabilizing Saturated Attitude Control in the Presence of Bounded Unknown Disturbances

Robert J. Wallsgrove* and Maruthi R. Akella†
University of Texas at Austin, Austin, Texas 78712

A smooth attitude-stabilizing control law is derived from which known limits on the control authority of the system are rigorously enforced. Unknown disturbance torques, assumed to be of lesser magnitude than the control limits, are included in the formulation. A smooth control signal containing hyperbolic tangent functions that rigorously obeys a known maximum-torque constraint is introduced. The controller can be viewed as a smooth analog of the variable-structure approach, with the degree of sharpness of the control permitted to vary with time according to a set of user-defined parameters. Lyapunov analysis is employed to ensure global stability, and asymptotic convergence of the angular velocity is guaranteed via the Barbalat lemma. Attitude errors, expressed as Euler parameters, are shown via simulation to vanish whenever certain design parameters are selected appropriately, and guidelines for selection of those parameters are provided in depth.

Introduction

RIGID-BODY attitude control is one of the more widely studied application areas within nonlinear control theory, largely because of its importance in robotics and spacecraft applications. These applications invariably involve practical design aspects that are difficult to include within theoretical studies but are nonetheless crucial to successful implementation of theoretical results. Two such aspects are 1) actuator saturation limits, which can lead to serious discrepancies between commanded input signals and actual control effort, and 2) disturbance signals, which always exist when knowledge of a system and its environment is incomplete.

Accounting for actuator saturation and/or external disturbances in nonlinear control systems has been the focus of tremendous research effort over the years. Extensive results pertaining to nominally linear systems containing actuator saturation nonlinearities are presented in Ref. 1 and references therein. Lyapunov-based design methods for robust nonlinear systems are developed in Ref. 2. One popular technique for handling disturbances is variable-structure control, which uses switching functions to attenuate disturbances, often by driving the system to a stable sliding mode.[3] The discontinuous nature of variable-structure and sliding-mode control designs is well known for exciting high-frequency unmodeled dynamics and for causing chattering, especially when applied to physical systems that are modeled imperfectly. Avoiding these pitfalls, commonly by using continuous approximations to switching functions, inevitably creates tradeoffs between theoretical performance guarantees and practicality.[4] Typical methods that account for chattering, notably the introduction of a boundary layer, sacrifice their asymptotic stability properties by allowing continuous control.[3]

Input saturation limits in spacecraft attitude control have been addressed in the literature by Tsiotras and Luo,[5] Di Gennaro,[6] Junkins et al.,[7] Robinett et al.,[8] and many others. Of particular interest is the recent work of Boskovic et al.[9] and of Akella and Kotamraju,[10] and Akella et al.[11] This paper presents a robust extension of the scheme introduced in Refs. 10 and 11, wherein smooth saturated control inputs are developed that guarantee asymptotic stability in the absence of disturbance torques. It also presents a smooth alternative to the controller in Ref. 9 with rigorous proof of various robustness and stability properties that is absent in that paper.

In Ref. 9, a variable-structure approach is used in conjunction with time-varying design elements to ensure global stability and robustness to disturbance torques with magnitudes of known upper bound. The control scheme in Ref. 9 guarantees that angular velocity error converges to the origin, whereas asymptotic convergence of the attitude error is possible through judicious choice of certain design parameters. What Ref. 9 lacks is theoretical proof that the continuous approximation to the variable-structure controller (via a boundary layer) retains the stability properties of the underlying discontinuous scheme. In contrast, the formulation in this paper uses continuous hyperbolic tangent functions, rather than the typical switching functions of variable-structure control, to guarantee boundedness of all closed-loop signals, convergence of the angular velocity error, and conformity with saturation limits. Furthermore, the control scheme developed here is flexible in that the degree of smoothness of the control (i.e., maximum rate of control input) is allowed to vary with time according to the needs of the application. The controller is completely independent of the inertia properties of the rigid body, a feature shared with most attitude-stabilizing controllers including the result given in Ref. 9.

The paper is organized as follows. The next section states the saturated attitude control problem. A solution is then presented in three parts: one that addresses the disturbance-free (i.e., nominal) case and two others that apply when bounded unknown disturbances are acting. Remarks on various novel aspects of the control scheme follow. Next the results of numerical simulations demonstrate various features of the proposed control law. Finally, the paper is completed with some concluding comments.

The notation

$$\|x\|_1 = \|x(t)\|_1 = \sum_{i=1}^{3} |x_i(t)|$$

where $x(t) \in \mathcal{R}^3$, refers to the pointwise 1-norm of vectors evaluated at a given instant, regardless of whether the argument (t) appears. The element-by-element hyperbolic tangent function is defined as $\mathrm{Tanh}(x) := [\tanh(x_1), \tanh(x_2), \tanh(x_3)]^T$. Lowercase italics are used for both real scalars and vectors in $\mathcal{R}^3$, and it is

Presented as AAS Paper 2004-0184 at the AAS/AIAA Space Flight Mechanics Winter Meeting, Maui, HI, 8–12 February 2004; received 12 April 2004; revision received 1 September 2004; accepted for publication 13 September 2004.

*Research Assistant, Department of Aerospace Engineering and Engineering Mechanics; rwallsgrove@mail.utexas.edu.

†Assistant Professor, Department of Aerospace Engineering and Engineering Mechanics, 1 University Station, Code C0600; makella@mail.utexas.edu. Member AIAA.

assumed that context distinguishes between the two cases wherever explicit definitions are not provided. Uppercase italics are used for the inertia matrix (J), Lyapunov candidate functions (V), and collections of terms that are introduced for brevity [A, C, and $V'^{(-)}_{\max}$].

Problem Statement

Attitude dynamics for a rigid body, represented with the familiar Euler parameters, are as follows[12]:

$$\dot{q}_0 = -\tfrac{1}{2} q^T \omega, \qquad \dot{q} = \tfrac{1}{2}(q_0 \omega + q \times \omega)$$

$$J\dot{\omega} = u + d - \omega \times J\omega \tag{1}$$

where $q(t)$ and $q_0(t)$ are the attitude quaternion vector and quaternion scalar, respectively; $\omega(t)$ is the angular velocity vector with respect to an inertial frame; J is the inertia matrix of the rigid body; and $u(t)$ and $d(t)$ are the control torque and disturbance torque, respectively. All three components of the control signal are constrained by a common maximum magnitude, expressed by

$$|u_i(t)| \le u_{\max}, \qquad \forall t \ge 0, \qquad i = 1, 2, 3 \tag{2}$$

and it is assumed that the control signal strictly dominates the unknown disturbance, that is,

$$|d_i(t)| \le d_{\max} < u_{\max}, \qquad \forall t \ge 0, \qquad i = 1, 2, 3 \tag{3}$$

Although state-dependent and time-varying saturation limits are of interest, for simplicity $d_{\max}$ and $u_{\max}$ are taken to be constants in the present formulation. Typical applications have a separate saturation limit $u_{\max(i)}$ for each component u_i, but a conservative common saturation limit $u_{\max} = \min_i[u_{\max(i)}]$ is adopted here to streamline the analysis. The attitude stabilization control objective is to find u subject to Eq. (2) such that for all initial conditions

$$q_0 \to \pm 1, \qquad q \to 0, \qquad \omega \to 0 \qquad \text{as} \qquad t \to \infty \tag{4}$$

Also fundamental to the control objective is that the control signal u has a bounded time derivative $\dot{u}$, so that possible excitation of high-frequency unmodeled dynamics is limited.

Note that the Euler parameters q and q_0 are defined with respect to an arbitrary nonrotating reference frame, and so the objective stated in Eq. (4) is equivalent to that of a set-point regulation problem.

Throughout the paper it is assumed that perfect measurements of q and ω are available, whereas no knowledge of d other than $d_{\max}$ is assumed.

Control Law Formulation

Assuming that attitude and angular velocity are measurements available for feedback, a control signal that satisfies Eq. (2) can be given by the sum of a proportional attitude (position) feedback term and a smooth switch-like mixed feedback term:

$$u = -\beta u_{\max} q - (1-\beta) u_{\max} \operatorname{Tanh}[(\omega + kq)/p^2]$$

$$0 < \beta < (1 - d_{\max}/u_{\max}) \le 1 \tag{5}$$

This control law is employed with an auxiliary time-varying attitude-gain function $k(t)$ that satisfies the following asymptotically stable first-order dynamics:

$$\dot{k} = -\gamma_k (1-\beta) u_{\max} q^T \{\operatorname{Tanh}[(\omega + kq)/p^2] + \operatorname{Tanh}(kq/p^2)\}$$

$$- \gamma_k \gamma_c k\left(q^T q + \gamma_d\right) \tag{6}$$

where $k(0) = k_0$ is an arbitrary scalar, γ_k and γ_d are positive scalar constants, and γ_c is simply a scaling/conversion factor that allows consistent physically meaningful units. In Eqs. (5) and (6), $p^2(t)$ is a nonzero scalar sharpness function that governs the magnitude of the control rates and is discussed in the following subsections. The form of Eq. (6) arises naturally from term cancellations in the Lyapunov stability analysis that follows. Other than the stabilizing terms on the far right, it is similar in structure to an analogous expression in Ref. 9.

The closed-loop stability analysis that follows is divided into three parts. Presented first is the stability proof for the disturbance-free nominal case, in which the sharpness function p^2 is subject to certain constraints and global asymptotic convergence is guaranteed. Next the effect of disturbances on the nominal controller is investigated. Finally a modified scheme is presented, in which the aforementioned constraints on p^2 are relaxed, and certain stability and convergence results are restored.

Part 1: Disturbance-Free Case ($d_{\max} = 0$)

In the absence of a disturbance torque, the control scheme in Eqs. (5) and (6) can be used with any upper-bounded continuous sharpness function p^2 that is bounded above zero:

$$0 < p^2_{\min} \le p^2 \in \mathcal{L}_\infty, \qquad \dot{p} \in \mathcal{L}_\infty \tag{7}$$

To establish that the resulting control scheme achieves the control objective, consider the following decrescent and radially unbounded Lyapunov function candidate:

$$V = \tfrac{1}{2}\omega^T J\omega + \beta u_{\max} q^T q + \beta u_{\max}(1-q_0)^2 + (1/2\gamma_k)k^2$$

$$= \tfrac{1}{2}\omega^T J\omega + 2\beta u_{\max}(1-q_0) + (1/2\gamma_k)k^2 \tag{8}$$

Differentiation of V with respect to time and substitution of the attitude dynamics from Eq. (1) yields the derivative $\dot{V} = \omega^T(u + \beta u_{\max} q) + k\dot{k}/\gamma_k$. Because V is decrescent and has continuous first partial derivatives with respect to the composite state $[\omega^T, q^T, (1-q_0), k]^T$, Lyapunov's stability theory dictates that the system is globally uniformly stable if this first time derivative is nonpositive for all time.[4] When further evaluated along Eqs. (5) and (6), $\dot{V}$ can be written in terms of $s = \omega + kq$ as

$$\dot{V} = -(1-\beta)u_{\max}[s^T \operatorname{Tanh}(s/p^2) + kq^T \operatorname{Tanh}(kq/p^2)]$$

$$- \gamma_c k^2\left(q^T q + \gamma_d\right) \le 0 \tag{9}$$

which implies that V, ω, and k are bounded for all time.

Because V is bounded and $x \tanh(|a|x) \ge 0$ for all a and x, integrating both sides of Eq. (9) with respect to time establishes integrability of $kq^T \operatorname{Tanh}(kq/p^2)$, and $s^T \operatorname{Tanh}(s/p^2)$:

$$V_\infty - V_0 \le -(1-\beta)u_{\max}\left[\int_0^\infty s^T \operatorname{Tanh}\left(\frac{s}{p^2}\right) \mathrm{d}t\right.$$

$$\left. + \int_0^\infty kq^T \operatorname{Tanh}\left(\frac{kq}{p^2}\right) \mathrm{d}t\right] \le 0 \tag{10}$$

Note that in Eq. (10) the symbols $V_\infty = \lim_{t\to\infty} V(t)$ and $V_0 = V(0)$ are used for brevity. Because the function $s^T \operatorname{Tanh}(s/p^2)$ is uniformly continuous and

$$\int_0^\infty s^T \operatorname{Tanh}\left(\frac{s}{p^2}\right) \mathrm{d}t$$

is finite, Barbalat's lemma dictates that $s = \omega + kq$ converges to the origin[13]:

$$s^T \operatorname{Tanh}(s/p^2) \to 0 \Rightarrow s \to 0 \tag{11}$$

Similarly, Barbalat's lemma can be used to show kq also converges to the origin because $kq^T \operatorname{Tanh}(kq/p^2)$ is uniformly continuous with a finite integral, so that

$$\left.\begin{aligned} \omega + kq &\to 0 \\ kq &\to 0 \end{aligned}\right\} \Rightarrow \omega \to 0 \tag{12}$$

At this point it remains to be shown that $q \to 0$ as $t \to \infty$. Convergence of kq to the origin in Eq. (12) leaves open the possibility that $k \to 0$ as $t \to \infty$ while q attains a nonzero value, which falls

short of the stated control objective. To rule out this possibility, recall the constraints of Eq. (7), and consider the time derivatives of ω. Boundedness of $\ddot{\omega}$ can be shown as follows:

$$\ddot{\omega} = J^{-1}(\dot{u} - \dot{\omega} \times J\omega - \omega \times J\dot{\omega})$$

$$\dot{u} = -\beta u_{\max}\dot{q} - (1-\beta)u_{\max}\frac{\mathrm{d}}{\mathrm{d}t}\,\mathrm{Tanh}\left(\frac{s}{p^2}\right)$$

$$\frac{\mathrm{d}}{\mathrm{d}t}\tanh\left(\frac{s_i}{p^2}\right) = \mathrm{sech}^2\left(\frac{s_i}{p^2}\right)\frac{[(\dot{\omega}_i + \dot{k}q_i + k\dot{q}_i)p - 2s_i\dot{p}]}{p^3}$$

$$\left.\begin{array}{r} 0 < p_{\min}^2 \le p^2 \\ \dot{p}, \dot{\omega}, \omega, \dot{q}, k, \dot{k} \in \mathcal{L}_\infty \end{array}\right\} \Rightarrow \left[\frac{\mathrm{d}}{\mathrm{d}t}\tanh\left(\frac{s_i}{p^2}\right) \in \mathcal{L}_\infty\right]$$
$$\Rightarrow (\dot{u} \in \mathcal{L}_\infty) \Rightarrow (\ddot{\omega} \in \mathcal{L}_\infty) \tag{13}$$

Equation (13) shows that because p^2 is restricted to be bounded above zero and uniformly continuous $\dot{\omega}$ is also uniformly continuous. From Barbalat's lemma, convergence of ω to the origin and uniform continuity of $\dot{\omega}$ together imply convergence of $\dot{\omega}$ to the origin, and so

$$(J\dot{\omega} \to 0) \Rightarrow (u \to 0) \Rightarrow (q \to 0) \tag{14}$$

Notice that this portion of the proof relies on the "leakage" term $\beta u_{\max} q$ in the control input of Eq. (5). Without it convergence of q to the origin cannot be guaranteed because zero-valued u and ω would not imply convergence of q to the origin. With β constrained to be nonzero and disturbance torques assumed absent, the attitude can be regulated successfully through the use of Eqs. (5) and (6) and any sharpness function p^2 that satisfies Eq. (7).

Part 2: Effect of Nonzero Disturbance Torques

The next step is to determine the effect of disturbance torques on the control law of Eqs. (5–7). To do so, consider the same Lyapunov function candidate as appears in Eq. (8), now subject to attitude dynamics containing an unknown disturbance torque d. Its derivative is given by $\dot{V} = \omega^T(u + d + \beta u_{\max} q) + k\dot{k}/\gamma_k$, which, when Eqs. (5) and (6) are applied, can be rewritten as

$$\dot{V} = \dot{V}_1 + \dot{V}_2 + \dot{V}_3$$
$$\dot{V}_1 = (\omega + kq)^T\left\{d - (1-\beta)u_{\max}\,\mathrm{Tanh}[(\omega + kq)/p^2]\right\}$$
$$\dot{V}_2 = -kq^T\left[d + (1-\beta)u_{\max}\,\mathrm{Tanh}(kq/p^2)\right]$$
$$\dot{V}_3 = -\gamma_c k^2 q^T q - \gamma_c\gamma_d k^2 \tag{15}$$

To establish bounds on the terms in Eq. (15), once again let $s = \omega + kq$, and consider the following inequality:

$$\dot{V}_1 = s^T\left[d - (1-\beta)u_{\max}\,\mathrm{Tanh}\left(\frac{s}{p^2}\right)\right]$$
$$= \sum_{i=1}^{3} s_i\left[d_i - (1-\beta)u_{\max}\tanh\left(\frac{s_i}{p^2}\right)\right]$$
$$\le \|s\|_1 d_{\max} - (1-\beta)u_{\max}\sum_{i=1}^{3}|s_i|\tanh\left(\frac{|s_i|}{p^2}\right)$$
$$= \|s\|_1 d_{\max} - (1-\beta)u_{\max}\sum_{i=1}^{3}|s_i|\tanh\left(\frac{|s_i|}{p^2}\right)$$
$$+ (1-\beta)u_{\max}\left(\sum_{i=1}^{3}|s_i| - \|s\|_1\right)$$
$$= \|s\|_1[d_{\max} - (1-\beta)u_{\max}]$$
$$+ (1-\beta)u_{\max}\sum_{i=1}^{3}\left\{|s_i|\left[1 - \tanh\left(\frac{|s_i|}{p^2}\right)\right]\right\} \tag{16}$$

By isolating the last term of this inequality and using algebraic features of the hyperbolic tangent function, one can introduce an upper bound that depends solely on the function p^2. Specifically, it can be shown that for all real scalars x and all nonzero real scalars y,

$$0 \le |x|(1 - \tanh|x/y|) \le \alpha|y| \tag{17}$$

where α is a positive constant with minimum value $\alpha^* = x^*(1 - \tanh x^*)$ for x^* satisfying $e^{-2x^*} + 1 - 2x^* = 0$. A simple algebraic analysis reveals that $\alpha^* < e^{-1}$, where e is the base of the natural logarithm. Using Eq. (17) in Eq. (16) with x and y replaced by s_i and p^2 respectively yields

$$\dot{V}_1 \le -A^2\|s\|_1 + 3\alpha(1-\beta)u_{\max}p^2$$
$$A^2 = (1-\beta)u_{\max} - d_{\max} > 0 \tag{18}$$

where $A^2 > 0$ as a result of the bounds on β given in Eq. (5). A procedure similar to that of Eqs. (16–18) applies to $\dot{V}_2$:

$$\dot{V}_2 \le -A^2\|kq\|_1 + 3\alpha(1-\beta)u_{\max}p^2 \tag{19}$$

Substituting Eqs. (18) and (19) into Eq. (15) reveals

$$\dot{V} \le -A^2(\|\omega + kq\|_1 + \|kq\|_1) - \gamma_c k^2\left(q^T q + \gamma_d\right) + C^2 p^2$$
$$C^2 = 6\alpha(1-\beta)u_{\max} > 0 \tag{20}$$

Notice that the first two terms in this upper bound are nonpositive, whereas the last is strictly positive and linearly dependent on the magnitude of the sharpness function p^2. Notice also that the negative terms in Eq. (20) decrease as $\|\omega\|_1$, $\|kq\|_1$, and k^2 increase. Because p^2 is upper bounded and the positive term has no dependence on the state, one can establish a residual error set to which $\|\omega\|_1$, $\|kq\|_1$, and k^2 must converge. Consider two upper bounds on $\dot{V}$ that follow from Eq. (20):

$$\dot{V} \le -A^2(\|\omega + kq\|_1 + \|kq\|_1) + C^2 p^2$$
$$\le -A^2\|\omega\|_1 + C^2 p^2 \tag{21}$$
$$\dot{V} \le -A^2\|kq\|_1 + C^2 p^2 \tag{22}$$

From these bounds it is clear that $\dot{V} < 0$ for all $\|\omega\|_1 > C^2A^{-2}p^2$ and all $\|kq\|_1 > C^2A^{-2}p^2$. Whenever $\|\omega\|_1$ or $\|kq\|_1$ become large, the negative terms in Eq. (20) dominate, making $\dot{V} < 0$ and drawing the state toward the origin. When $\|\omega\|_1$ and $\|kq\|_1$ reach sufficiently small values (determined by p^2), the sign of $\dot{V}$ is indefinite, and progress toward the origin cannot be guaranteed. These critical sizes of ω and kq represent the boundary of a residual error set to which all trajectories will eventually converge; therefore, ω and kq are globally bounded. Furthermore q is necessarily bounded by the quaternion constraint $\|q\|_2^2 + q_0^2 = 1$, and boundedness of k follows directly from the expression for $\dot{k}$ in Eq. (6):

$$\frac{\mathrm{d}}{\mathrm{d}t}\left(\frac{1}{2}k^2\right) = -\gamma_k(1-\beta)u_{\max}kq^T\left[\mathrm{Tanh}\left(\frac{s}{p^2}\right) + \mathrm{Tanh}\left(\frac{kq}{p^2}\right)\right]$$
$$- \gamma_k\gamma_c\left(\gamma_d + q^T q\right)k^2$$
$$\le \gamma_k 2\sqrt{3}(1-\beta)u_{\max}|k| - \gamma_k\gamma_c\gamma_d k^2$$
$$\le -\frac{\gamma_k\gamma_c\gamma_d}{2}\left\{k^2 - \left[\frac{2\sqrt{3}(1-\beta)u_{\max}}{\gamma_c\gamma_d}\right]^2\right\} \tag{23}$$

Equation (23) ensures that $|k|$ decreases whenever it exceeds a certain critical value determined by the parameters of the problem. Global boundedness of k and ω is therefore guaranteed, but no claims of asymptotic convergence can be made for either ω or q.

Notice that reducing the value of p^2 diminishes the size of the aforementioned residual error set to which ω and kq converge, which brings the eventual state of the closed-loop system closer to the origin. In the following section this feature is exploited to derive a more effective sharpness function p^2 that allows better robustness to disturbance torques.

Part 3: Disturbance-Accommodating Modification

The preceding developments have shown that when the constraints in Eq. (7) are in place the addition of disturbance torques prevents global asymptotic stability. Alternatively, the control in Eqs. (5) and (6) can be used with a sharpness function p^2 of the form

$$p^2(t) = p_0^2 e^{-\gamma_p C^2 t} + \gamma_p \gamma_c \int_0^t \exp\left[-\gamma_p C^2 (t-\sigma)\right] k(\sigma)^2 \times \left[q(\sigma)^T q(\sigma) + \gamma_d\right] \mathrm{d}\sigma \tag{24}$$

which is nonnegative for all $t \geq 0$ and nonzero for all finite t provided $p^2(0) = p_0^2$ is nonzero. Here γ_p is a positive scalar constant. The requirement that p^2 be strictly bounded above zero has been removed, and p^2 in Eq. (24) can be easily identified as the solution to the stable linear differential equation

$$\frac{\mathrm{d}}{\mathrm{d}t}(p^2) = -\gamma_p C^2 p^2 + \gamma_p \gamma_c k^2 \left(q^T q + \gamma_d\right) \tag{25}$$

Equation (25) motivates the choice for p^2 in Eq. (24) because it allows important term cancellations in the Lyapunov analysis that follows. The symbol p^2 has been used to make clear that the function is nonnegative.

Now consider a modified decrescent and radially unbounded Lyapunov function candidate and its first time derivative:

$$V = \frac{1}{2}\omega^T J \omega + 2\beta u_{\max}(1 - q_0) + \frac{1}{2\gamma_k}k^2 + \frac{1}{\gamma_p}p^2$$

$$\dot{V} = \omega^T (u + d + \beta u_{\max} q) + \frac{1}{\gamma_k} k\dot{k} + \frac{1}{\gamma_p}\frac{\mathrm{d}}{\mathrm{d}t}(p^2) \tag{26}$$

When Eqs. (5) and (6) are applied, the Lyapunov derivative in Eq. (26) can be algebraically rearranged in steps identical to those employed in deriving Eq. (15), namely,

$$\dot{V} = \dot{V}_1 + \dot{V}_2 + \dot{V}_3$$

$$\dot{V}_1 = s^T \left[d - (1-\beta)u_{\max} \operatorname{Tanh}(s/p^2)\right]$$

$$\dot{V}_2 = -kq^T \left[d + (1-\beta)u_{\max} \operatorname{Tanh}(kq/p^2)\right]$$

$$\dot{V}_3 = -6\alpha(1-\beta)u_{\max} p^2 \tag{27}$$

Repeating the steps of Eqs. (16–19) yields

$$\dot{V}_1 \leq \|s\|_1 [d_{\max} - (1-\beta)u_{\max}] + 3\alpha(1-\beta)u_{\max} p^2$$

$$\dot{V}_2 \leq \|kq\|_1 [d_{\max} - (1-\beta)u_{\max}] + 3\alpha(1-\beta)u_{\max} p^2 \tag{28}$$

so that $\dot{V} \leq -A^2(\|\omega + kq\|_1 + \|kq\|_1) \leq 0$; therefore, V, ω, k, and p are uniformly bounded, which implies $\mathcal{L}_1$ integrability of ω and kq:

$$-A^{-2}(V_\infty - V_0) \geq \int_0^\infty \|\omega + kq\|_1 \,\mathrm{d}t + \int_0^\infty \|kq\|_1 \,\mathrm{d}t \geq \int_0^\infty \|\omega\|_1 \,\mathrm{d}t \tag{29}$$

Now $\|\omega\|_1$ and $\|kq\|_1$ are uniformly continuous functions with finite integrals over $[0\ \infty)$, so that Barbalat's lemma applies and

$$\lim_{t\to\infty} \omega = 0, \qquad \lim_{t\to\infty} kq = 0 \tag{30}$$

Notice that removing the lower-bound constraint on p^2 in Eq. (7) has shrunk the residual error set just discussed to allow asymptotic convergence of ω and kq. Meeting the overall control objective therefore reduces to showing that $(kq \to 0) \Rightarrow (q \to 0)$, meaning that k does not converge to zero unless q converges to the origin. Although no explicit guarantee that q converges can be made in this case, it is clear that proper selection of k_0, γ_k, and γ_d can result in k converging more slowly than q does. The following section discusses how to choose these parameters to increase the likelihood that q converges to the origin as $t \to \infty$.

Discussion

Close inspection of the formulation described in Eqs. (5) and (6) illuminates several novel features of the both the original, that is, Eq. (7), and the modified, that is, Eq. (24), control schemes.

Compliance with Saturation Constraint

The bounded nature of Euler parameters and the hyperbolic tangent function (i.e., $|q_i| \leq 1$ and $|\tanh(\cdot)| \leq 1$), along with the chosen bounds on the parameter β, ensure that the control law in Eq. (5) satisfies the saturation limits in Eq. (2):

$$|u_i| \leq |\beta u_{\max} q_i| + \left|(1-\beta)u_{\max} \tanh\left(s_i \big/ p^2\right)\right| \leq \beta u_{\max} + (1-\beta)u_{\max} = u_{\max} \tag{31}$$

Role of Sharpness Function p^2

Equation (5) makes clear the role of the sharpness function p^2 in the controller operation. It appears in the denominator of the argument of the hyperbolic tangent function, so that its value at any given time determines how strongly the control varies with the signal $\omega + kq$. If p^2 decreases, $\|\dot{u}\|$ can take on higher values so that the control more closely resembles a switching function. In the original scheme p^2 can be freely defined [respecting Eq. (7)] according to the needs of the application. If errors are very small or high control rates are allowable, then low values of p^2 can be used; otherwise, increasing p^2 can temper the control response to avoid high-frequency excitation. In the disturbance-accommodating modified scheme, the sharpness characteristics of the control can be set via selection of parameters p_0^2 and γ_p. Adjusting p_0^2 changes the rate of change of the control torque during the initial phases of stabilization, in which angular velocity is typically largest. By selecting γ_p, one can choose how quickly the sharpness of the control signal changes. It is important to observe Eq. (25) and note that p^2 is the solution to a stable linear differential equation forced by the bounded signals $k^2 q^T q$ and k^2, so that convergence of those signals to zero can cause p^2 to approach zero over time. Note also that p^2 appears in Eq. (6), where it determines how strongly $\dot{k}$ varies with the angular velocity and attitude errors.

Role of Attitude Gain k

In both the original and modified schemes, the time-varying attitude gain k appears as a scaling factor on the attitude quaternion vector, so that higher k values serve to shift the emphasis of the control from ω to q. This makes clear the importance of avoiding convergence of k to zero while q is nonzero: zero-valued k implies greatly diminished control response to attitude errors. Selection of γ_k affects how quickly k changes, while γ_d determines the relative importance of the linear proportional term in Eq. (6). Note that the term involving γ_d tends to drive k to zero, so that selection of small γ_d values is typically preferable to large ones. Simulations have shown that in most cases sufficiently large $|k_0|$ and/or sufficiently small γ_k and γ_d can be found which ensure that the attitude converges to the origin in spite of disturbances (see the following section for an example). Regardless of whether disturbances are present, proper selection of these parameters is necessary to "tune" the controller for acceptable performance.

Another important feature of k is that its derivative in Eq. (6) contains the attitude error q, meaning that inclusion of dynamic gain k increases the order of the closed-loop system from seven to eight. Note that when errors are small the hyperbolic tangent terms in Eq. (5) are approximately linear in their arguments, and if a constant $k = k_0$ is used the controller resembles a proportional/derivative (PD) feedback scheme in which k_0 is the proportional gain. Instead, the internal dynamics of k introduce an integrator effect that makes u resemble a proportional/integral/derivative scheme, rather than a simple PD. Inclusion of dynamic-state feedback in this manner is well known to diminish steady-state errors and aid in disturbance rejection in general set-point regulation problems that include parameter uncertainty and/or modeled disturbances.[14] Advantages associated with using dynamic-state feedback are also apparent in tracking applications that involve exogenous reference models.[15]

Role of Leakage Parameter β

A leakage parameter β also appears in Eqs. (5), the value of which determines the relative importance of the direct attitude feedback term and the switch-like hyperbolic tangent term. Lower β values are generally more desirable than higher ones because $\dot{V}$ is bounded above by negative terms proportional to $(1-\beta)$. On the other hand, in situations where k is prone to convergence to zero (e.g., small $|k_0|$, large γ_k, and/or large γ_d) higher β values can shift the focus of control toward the attitude error rather than the angular velocity, which can help promote convergence of q in exchange for slower overall closed-loop performance. Recall that the stability proof in the disturbance-free case relies crucially on β being nonzero.

Continuity of Control Torque

Throughout the formulation the expression for the control torque u and the differential equation for the attitude gain rate $\dot{k}$ remain unchanged, so that the only difference between the solutions for the disturbance-free and nonzero-disturbance cases is the nature of the sharpness function p^2. When external disturbances are absent, the control is effective with any upper-bounded p^2 provided it is strictly bounded above zero. Requiring $0 < p^2_{\min} \le p^2$ imposes a rate limit on the control torque, which is advantageous in avoiding high-frequency dynamic excitation. Although nonzero-bounded disturbances do not cause instability in this scheme, asymptotic stability in the presence of disturbance torques hinges on allowing p^2 to gradually approach zero over time, which admits the possibility of infinitely fast changes in the control signal in the limit as $t \to \infty$.

When the sharpness parameter p^2 is allowed to approach zero, at first glance it appears that the control in Eq. (5) is likely to excite high-frequency modes when applied to flexible spacecraft. This is not necessarily always the case because an important aspect of the formulation is that the sum $\omega + kq$ also approaches the origin, potentially at a rate comparable to that of p^2. The result is that although the scheme has the capacity for infinite torque rates (in the limit as $t \to \infty$) the control signal is only as sharp as it needs to be to counteract the time-varying external disturbance. Note that at no point in the stability proof is it assumed that the disturbance has bounded derivative. To offset disturbances with high-frequency components, the control torque must be able to change at least as rapidly as the disturbance does, and the controller presented here (when properly tuned) does not introduce high-frequency signals unless they are already acting on the spacecraft through the disturbance.

What is most important is that u has possibly unbounded rates only in the limit as $t \to \infty$, and the maximum rate of decay of p^2 can be set via selection of various parameters, notably γ_p; therefore, it is reasonable to expect acceptable torque rates throughout the operational period of the controller given proper parameter selection.

Comparison to Variable-Structure Control

For very small β, the controller presented here can be regarded as analogous to a variable structure scheme in which the smoothness of the control is allowed to vary with time. In nominal operation (i.e., zero disturbances), the smoothness can be freely user defined via the sharpness function p^2 to match the needs of the application, provided upper and lower bounds are maintained. Successful disturbance attenuation (beyond mere stability) requires that p^2 satisfies Eq. (24), but the sharpness function nonetheless contains free parameters that can be selected to tailor the smoothness of the control to the needs of the user. This ability to adjust the degree of smoothness of the control signal is a primary advantage of this control law and a significant improvement from the variable-structure results in Ref. 9 and elsewhere.

Simulations

To demonstrate the features of the control scheme in Eqs. (5) and (6), several simulations were performed with a standard explicit Runge–Kutta $\frac{4}{5}$ numerical integration scheme employing the algorithm in Ref. 16. Relative and absolute error tolerances were set at 10^{-7} throughout the simulations.

The simulations are applied to a rigid spacecraft with the following inertia matrix:

$$J = \begin{bmatrix} 22 & 1 & 3 \\ 1 & 19 & 2 \\ 3 & 2 & 25 \end{bmatrix} \text{ kg m}^2 \tag{32}$$

The spacecraft can apply a maximum control torque $u_{\max} = 20$ N m about each axis. In the simulated scenario the spacecraft starts with angular velocity $\omega = [-90.0, 135, 67.5]^T$ deg/s, initially rotated 73.74 deg about the axis $[\frac{2}{3}, \frac{1}{3}, -\frac{2}{3}]^T$, so that $q_0 = 0.8$ and $q = [0.4, 0.2, -0.4]^T$ at the simulation start time.

Figures 1–5 show the results of several simulations, the specific features of which are described in the following subsections. Note that in the bottom panes of Figs. 3 and 4 the following notation is used for clarity:

$$V'^{(-)}_{\max} = -A^2(\|\omega + kq\|_1 + \|kq\|_1) - \gamma_c k^2\left(q^T q + \gamma_d\right) \tag{33}$$

The function $V'^{(-)}_{\max}$ contains the negative terms in the upper bound on $\dot{V}$ given in Eq. (20). Note also that units are not labeled in the figures; instead, the standard units listed here have been used in all plots: ω, k (rad/s); u, d (N m); p^2 (s^{-1}); t (s); $\dot{u}$, $V'^{(-)}_{\max}$ (N m s^{-1}). Table 1 lists parameter values that are used in all simulations.

Nominal Performance

The roles of auxiliary functions k and p^2 are demonstrated via Figs. 1 and 2 for the disturbance-free nominal case.

In the simulation shown in Fig. 1, the original controller of Eqs. (5–7) is applied twice with different sharpness parameters (constant p^2) to demonstrate the effect of changes in p^2. An initial attitude gain $k_0 = 2$ rad/s was used for both simulations shown in Fig. 1.

Figure 1 shows how the value of p^2 affects the sharpness of the control response: increasing p^2 smoothes the control signal and decreases control rates but slows the closed-loop convergence rates.

Changing the design parameters associated with the time-varying attitude gain k also affects how the controller in Eq. (5) performs. Figure 2 shows the results of three simulations in which p^2 is fixed at 1 s^{-1} and k_0 is given three different values.

Table 1 Parameter values for Figs. 1–5

Parameter	Value
α	0.2785
β	5×10^{-4}
γ_k, rad kg^{-1} m^{-2}	10^{-3}
γ_d	10^{-5}
γ_c, kg m^2 s^{-1}	1

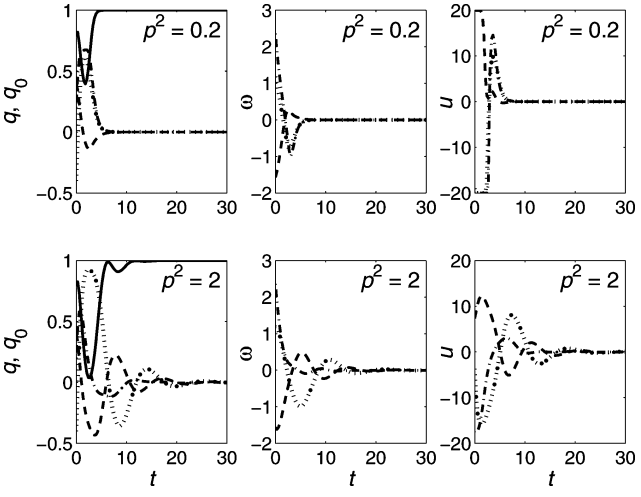

Fig. 1 Disturbance-free performance for two values of p^2.

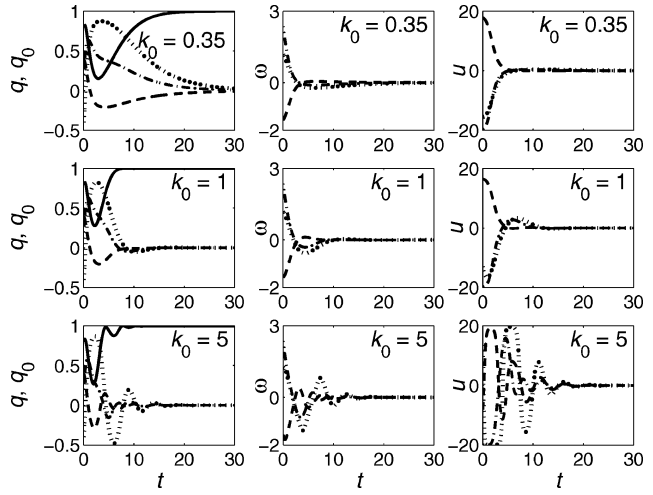

Fig. 2 Disturbance-free performance for three values of k_0.

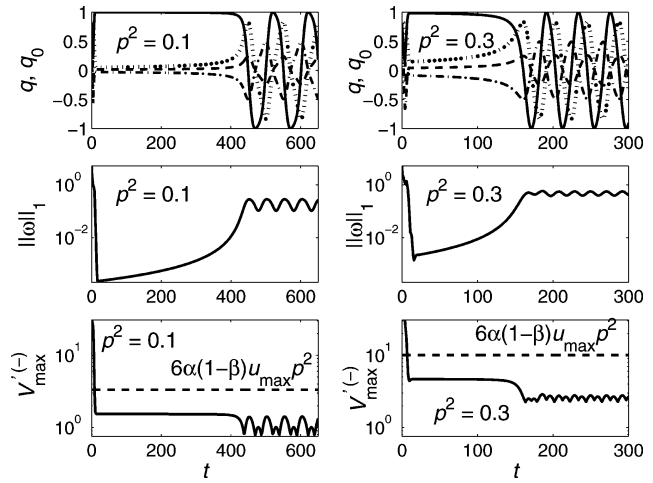

Fig. 3 Original controller performance under constant disturbance for two values of p^2.

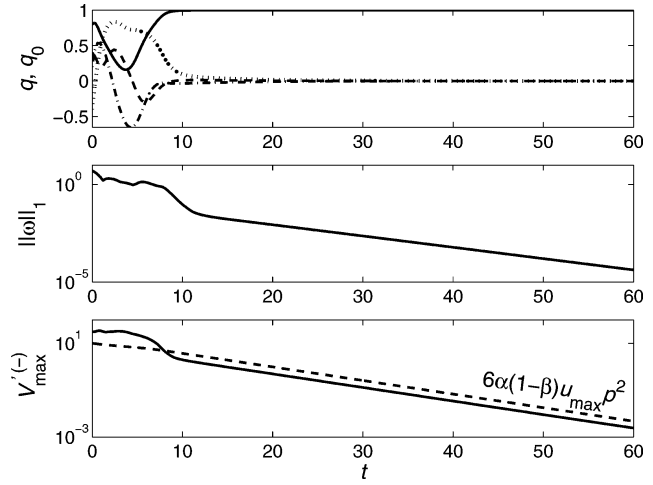

Fig. 4 Modified controller performance under constant disturbance (compare to Fig. 3).

Interpreted in the language of the classic second-order linear system, a higher k value corresponds conceptually to a lower damping ratio. When k_0 is increased, the emphasis of the control is shifted away from the derivative term (i.e., ω) and toward the proportional term (i.e., q), which results in the "underdamped" oscillatory behavior seen in the lower portion of Fig. 2. Likewise when k_0 is decreased the closed-loop system exhibits the slow overdamped behavior apparent in the top row of Fig. 2. Increasing k_0 provides an increased response to attitude errors that is vital to the control objective, but k_0 (and γ_k) must be selected appropriately to tune the controller and avoid both the sluggish behavior and the wild oscillations seen in Fig. 2.

Table 2 Parameter values for Fig. 5

Parameter	Value
k_0, rad/s	2
p_0^2, s^{-1}	1
γ_p, $kg^{-1}\ m^{-2}\ s$	4×10^{-3}

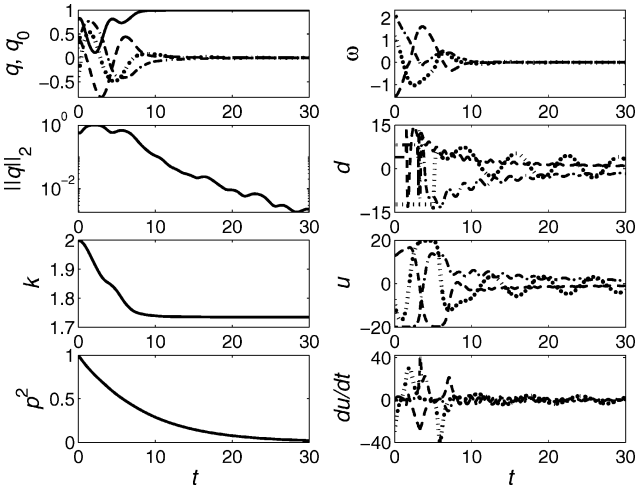

Fig. 5 Performance of modified controller under general disturbance.

Performance Under Disturbance Torques: Original Scheme

It has been shown that the presence of nonzero disturbance torques disrupts the asymptotic convergence properties of the original controller subject to Eq. (7). In this case the value of p^2 determines the size of a residual error set to which attitude and angular velocity errors ultimately converge. This feature is demonstrated via the simulations shown in Fig. 3. The spacecraft is subjected to constant disturbance torque $d = [4.5, -9, 13.5]^T$ N m, whereas the maximum disturbance value is taken to be $d_{\max} = 15$ N m. The initial attitude gain was set to $k_0 = 2$ rad/s for both simulations pictured in Fig. 3.

Although the unmodified controller is unable to regulate the attitude under disturbances, it does bring the angular velocity and attitude errors [shown as $\|\omega\|_1$ and $V'^{(-)}_{\max}$] to within the expected neighborhood of the origin, where they remain indefinitely. Figure 3 makes clear the relationship between the sharpness factor p^2 and the size of the residual error set: lower values of p^2 correspond to smaller steady-state angular velocity errors.

Performance Under Disturbance Torques: Modified Scheme

Robustness of the modified controller in Eqs. (5), (6), and (24) to bounded unknown disturbances is demonstrated in the following simulations.

The first simulation scenario is identical to the one shown in Fig. 3, except that p^2 is allowed to vary in accordance with Eq. (24). Figure 4 shows the results when the modified controller is applied with $p_0^2 = 0.3\ s^{-1}$ and $\gamma_p = 4 \times 10^{-3}\ kg^{-1}\ m^{-2}\ s$.

As expected, allowing p^2 to approach zero in the modified controller shrinks the residual error sets seen in Fig. 4 so that asymptotic convergence is possible.

A final simulation is included to demonstrate all aspects of the control scheme when applied in the presence of general time-varying disturbances. In the final simulation the spacecraft is subjected to unknown disturbances of maximum magnitude $d_{\max} = 15$ N m with

Table 3 Disturbance settings for Fig. 5

i	a_i, N·m	b_i, s	c_i, s	f_i, N·m	g_i, s^{-1}	h_i, s^{-1}	m_i	t_{io}, s	d_{io}, N·m
1	13.5	$8\pi/7$	−1.273	1.5	0.10	2π	$-\pi/2$	1.5	3.98
2	−12.0	$2\pi/3$	−2.840	3.0	0.10	π	$-\pi/2$	3.0	8.21
3	10.5	$2\pi/5$	−4.760	−4.5	0.01	$3\pi/10$	$-5\pi/4$	5.0	−12.28

components of the form

$$d_i(t) = d_{io}, \qquad t \le t_{io}, \qquad i = 1, 2, 3$$

$$d_i(t) = a_i \sin\left[b_i(t + c_i)^{-1}\right] + f_i \exp[-|g_i|(t - t_{io})] \sin(h_i t + m_i), \qquad t > t_{io} \tag{34}$$

where $|a_i| + |f_i| = d_{max}$, $c_i \ge -t_{io}$, and $d_{io} \in [-d_{max}, d_{max}]$ is a constant initial torque value. The signal described by Eq. (34) is intended to mimic a disturbance process with high initial rates (e.g., noisy transient behavior) that eventually converges to a lower-frequency time-varying steady-state signal. Figure 5 shows the performance of the controller when this disturbance is acting, and the design parameters are set at the values listed in Table 2. Note that the disturbance signal given by Eq. (34), with the parameters listed in Table 3, is plotted in the right column and second row from the top of Fig. 5.

Figure 5 shows that the control signal swings away from its saturation limits during the initial phases of operation (high ω) and smoothly transitions to a disturbance-tracking mode as time increases. The control rates can be seen in Fig. 5 to be reasonable: they do not increase dramatically as $p^2 \to 0$. Indeed the control takes on high rates only when the disturbance is of high frequency. Although the unbounded nature of p^{-2} gives rise to numerical problems in simulations of long duration, the case shown here has been seen to converge to $\|q\|_2 < 10^{-6}$ within 80 s, by which time $p^2 \approx 3 \times 10^{-5}$ s^{-1}.

Conclusions

Attitude control systems for current and future spacecraft, including the Next-Generation Space Telescope and space-based lasers among others, are subject to increasingly stringent performance requirements. Many of these spacecraft also rely on deployable appendages and sparse structural layout, which make them increasingly flexible and susceptible to high-frequency dynamic excitation. This paper is motivated by the need for precise spacecraft attitude control techniques that account for actuator saturation in the presence of unmeasured disturbances without exciting high-frequency dynamics. By allowing smooth control without sacrificing stability results, the proposed approach meets that need.

The primary contribution of this work is a rigorous theoretical proof that a smooth control signal with time-varying sharpness can be used to offset the disadvantages of existing saturation-respecting controllers. The concept replaces the ad hoc approximate sign functions and boundary layers commonly introduced to avoid those disadvantages in the current literature. Unlike existing attempts to use continuous control to this end, the approach presented here provides truly global results backed up by a complete stability proof. Angular velocity errors are guaranteed to vanish in the presence of disturbances regardless of parameter selections or features of the maneuver. Although asymptotic convergence of the attitude error to the origin is not ensured in this case, practical design guidelines are shown to be effective in regulating residual orientation errors. The only significant limitation apparent in this formulation is the need for the sharpness function to approach zero over time, which is fundamental to the goal of completely rejecting arbitrary bounded disturbances: analogous limitations exist in all comparable formulations available in existing literature.

The formulation presented in this paper is a particular manifestation of the variable-smoothness control concept, and many alternate formulations are possible. The novel ideas of a sharpness function and a dynamic attitude gain are desirable in terms of their analytical features and simulated performance, but the expressions used here to implement those ideas could potentially be modified without sacrificing any of the stability results. Likewise the use of hyperbolic tangent functions, although fundamental to the structure of this formulation, might be just one among many ways to implement the underlying concepts for saturated attitude control.

Acknowledgments

These results are based in part on work supported by the Texas Advanced Research Program under Grant 003658-0081-2001. The authors offer thanks to the Air Force Research Laboratories' Space Scholars Program for its help in motivating this work. Thanks are also extended to the W. M. Keck Foundation for its support of the Thrust 2000 Endowed Graduate Fellowship Program.

References

[1]Hu, T., and Lin, Z., *Control Systems with Actuator Saturation*, Birkhäuser, Boston, 2001, pp. 55–325.

[2]Freeman, R. A., and Kokotvic, P., *Robust Nonlinear Control Design*, Birkhäuser, Boston, 1996, pp. 33–227.

[3]DeCarlo, R. A., Zak, S. H., and Drakunov, S. V., "Variable Structure Sliding-Mode Controller Design," *Control Handbook*, edited by W. S. Levine, CRC Press, Boca Raton, FL, 1996, pp. 941–951.

[4]Slotine, J. J. E., and Li, W., *Applied Nonlinear Control*, Prentice–Hall, Upper Saddle River, NJ, 1991, pp. 57–96, 276–306.

[5]Tsiotras, P., and Luo, J., "Control of Underactuated Spacecraft with Bounded Inputs," *Automatica*, Vol. 36, No. 8, 2000, pp. 1153–1169.

[6]Di Gennaro, S., "Stabilization of Rigid Spacecraft with Uncertainties and Input Saturation in a Central Gravitational Field," *Proceedings of the 36th Conference on Decision and Control*, Vol. 5, 1997, pp. 4204–4209.

[7]Junkins, J. L., Akella, M. R., and Robinett, R. D., "Nonlinear Adaptive Control of Spacecraft Maneuvers," *Journal of Guidance, Control, and Dynamics*, Vol. 20, No. 6, 1997, pp. 1104–1110.

[8]Robinett, R. D., Parker, G. D., Schaub, H., and Junkins, J. L., "Lyapunov Optimal Saturated Control for Nonlinear Systems," *Journal of Guidance, Control, and Dynamics*, Vol. 20, No. 6, 1997, pp. 1083–1088.

[9]Boskovic, J. D., Li, S. M., and Mehra, R. K., "Robust Adaptive Variable Structure Control of Spacecraft Under Control Input Saturation," *Journal of Guidance, Control, and Dynamics*, Vol. 24, No. 1, 2001, pp. 14–22.

[10]Akella, M. R., and Kotamraju, G. R., "Spacecraft Attitude Control in the Presence of Actuator Magnitude and Rate Saturation Limits," *14th U.S. Congress on Theoretical and Applied Mechanics*, Virginia Polytechnic Inst. and State Univ., Blacksburg, VA, June 2002.

[11]Akella, M. R., Valdivia, A., and Kotamraju, G. R., "Velocity-Free Attitude Controllers Subject to Actuator Magnitude and Rate Saturations," *Journal of Guidance, Control, and Dynamics* (to be published).

[12]Wie, B., *Space Vehicle Dynamics and Control*, AIAA, Reston, VA, 1998, pp. 326, 327.

[13]Popov, V. M., *Hyperstability of Control Systems*, Springer-Verlag, New York, 1973, p. 211.

[14]Khalil, H. K., *Nonlinear Systems*, Prentice–Hall, Upper Saddle River, NJ, 2002, pp. 469–499.

[15]Isidori, A., *Nonlinear Control Systems*, Springer-Verlag, London, 1995, pp. 178–184.

[16]Dormand, J. R., and Prince, P. J., "A Family of Embedded Runge–Kutta Formulae," *Journal of Computational and Applied Mathematics*, Vol. 6, No. 1, 1980, pp. 19–26.